An adaptive finite element method for the wave equation based on anisotropic a posteriori error estimates in the $L^2(H^1)$ norm

Marco Picasso

INSTITUT NATIONAL DE RECHERCHE EN INFORMATIQUE ET EN AUTOMATIQUE

An adaptive finite element method for the wave equation based on anisotropic a posteriori error estimates in the $L^2(H^1)$ norm.

Marco Picasso

N° 7115

Novembre 2009

Domaine 1

apport de recherche

ISSN 0249-6399 ISRN INRIA/RR--7115--FR+ENG

INSTITUT NATIONAL
DE RECHERCHE
EN INFORMATIQUE
ET EN AUTOMATIQUE

INRIA

centre de recherche
PARIS - ROCQUENCOURT

An adaptive finite element method for the wave equation based on anisotropic a posteriori error estimates in the $L^2(H^1)$ norm.

Marco Picasso

Domaine : Mathématiques appliquées, calcul et simulation
Équipe-Projet Gamma

Rapport de recherche n° 7115 — Novembre 2009 — 22 pages

Abstract: An adaptive finite element algorithm is presented for the wave equation in two space dimensions. The goal of the adaptive algorithm is to control the error in the same norm as for parabolic problems, namely the $L^2(0,T;H^1(\Omega))$ norm, where T denotes the final time and Ω the computational domain. The mesh aspect ratio can be large whenever needed, thus allowing a given level of accuracy to be reached with fewer vertices than with classical isotropic meshes. The refinement and coarsening criteria are based on anisotropic, a posteriori error estimates and on an elliptic reconstruction.

A numerical study of the effectivity index on non-adapted meshes confirms the sharpness of the error estimator. Numerical results on adapted meshes indicate that the error indicator slightly underestimates the true error. We conjecture that the missing information corresponds to the interpolation error between successive meshes. It is observed that the error indicator becomes sharp again when considering the damped wave equation with a large damping coefficient, thus when the parabolic character of the PDE becomes predominant.

Key-words: Wave equation, Adaptive finite elements, Anisotropic a posteriori error estimates

Centre de recherche INRIA Paris – Rocquencourt
Domaine de Voluceau, Rocquencourt, BP 105, 78153 Le Chesnay Cedex
Téléphone : +33 1 39 63 55 11 — Télécopie : +33 1 39 63 53 30

Un algorithme de maillage adaptatif pour l'équation des ondes basé sur des estimations d'erreur a posteriori anisotropes dans la norme $L^2(H^1)$.

Résumé : Un algorithme d'éléments finis adaptatifs est présenté pour l'équation des ondes à deux dimensions d'espace. Le but de l'algorithme est de contrôler l'erreur dans la norme naturelle des problèmes paraboliques, à savoir la norme $L^2(0,T;H^1(\Omega))$. Le rapport d'aspect des triangles peut être grand si nécessaire, ce qui permet d'obtenir un niveau de précision donné avec relativement peu de sommets. Les critères de raffinement et déraffinement sont basés sur un estimateur d'erreur a posteriori anisotrope.

Les résultats numériques sur des maillages non-adaptés montrent que l'estimateur d'erreur est précis. Les résultats numériques sur des maillages adaptés montrent que l'estimateur d'erreur sous-estime légèrement l'erreur. Nous pensons que cette discrépance provient de l'erreur d'interpolation entre maillages qui n'est pas contenue dans l'estimateur. Les résultats montrent que cette erreur d'interpolation entre maillages dimunue lorsqu'un terme d'amortissement est ajouté dans l'équation des ondes, c'est-à-dire lorsque le caractère parabolique de l'équation augmente.

Mots-clés : Equation des ondes, Eléments finis adaptatifs, Estimations d'erreur a posteriori anisotropes

1 Introduction

A posteriori error estimates and adaptive finite elements have already been widely considered for solving elliptic, parabolic and first order hyperbolic problems. However, hyperbolic problems of second order have been much less studied, see for instance [15, 5, 6, 1, 2, 8].

Recently, adaptive finite elements with large aspect ratio have been introduced in order to reduce the number of vertices required for a given level of accuracy [3, 7]. Elliptic problems were considered in [21, 22], with goal to control the error in the natural $H^1(\Omega)$ norm, while the $L^2(0,T;H^1(\Omega))$ norm was used for parabolic problems in [20, 10, 17].

When considering hyperbolic problems of second order, the natural norm is the $\mathcal{C}^0([0,T];H_0^1(\Omega)) \cap \mathcal{C}^1([0,T];L^2(\Omega))$ norm. However, as explained in [8], the $\mathcal{C}^0([0,T];L^2(\Omega)) \cap \mathcal{C}^1([0,T];H^{-1}(\Omega))$ norm seems to be more appropriate in order to derive a posteriori error estimates.

In this paper, a posteriori error estimates are derived in the $L^2(0,T;H^1(\Omega))$ norm for the wave equation in two space dimensions, which allows the adaptive algorithms developed for parabolic problems in [20, 10, 17] to be used with very few modifications. For this purpose, the elliptic reconstruction technique [18] introduced for parabolic problems will be used.

The outline is the following. The wave equation and the continuous, piecewise linear finite element discretization in space is presented in the next section. An a posteriori upper bound is proposed in section 3 for the error in the $L^2(0,T;H^1(\Omega))$ norm, using the elliptic reconstruction technique introduced for parabolic problems in [18]. An order two time discretization is selected and numerical results on non-adapted meshes are reported in section 4. It is observed that the error indicator is sharp provided the error due to time discretization becomes negligible, which is the case when the time step τ is of the order of the space step h. An adaptive algorithm is presented in section 5 in order to control the error in the $L^2(0,T;H^1(\Omega))$ norm. Numerical results show a discrepancy between the error indicator and the true error. We suspect that this discrepancy corresponds to the interpolation error between successive meshes which is not accounted in the present paper - and difficult to compute since non-compatible anisotropic meshes are involved. In order to validate this conjecture, the adaptive algorithm is used to solve the damped wave equation. It is observed that the larger the damping term, the better the effectivity index. This observation is consistent with the fact that we have observed in previous papers [20, 10, 17] that the interpolation error between successive meshes was not relevant for parabolic problems. We therefore conclude that this is not true for the wave equation.

2 The wave equation and its finite element discretization

Let T be the final time, let Ω be a polygon. Given $f : \Omega \times (0,T) \to \mathbb{R}$, given initial conditions $u_0, v_0 : \Omega \to \mathbb{R}$, we are interested in finding $u : \Omega \times (0,T) \to \mathbb{R}$

such that

$$\frac{\partial^2 u}{\partial t^2} - \Delta u = f \qquad \text{in } \Omega \times (0,T), \tag{1}$$

$$u = 0 \qquad \text{on } \partial\Omega \times (0,T), \tag{2}$$

$$u(\cdot,0) = u_0, \quad \frac{\partial u}{\partial t}(\cdot,0) = v_0 \qquad \text{in } \Omega. \tag{3}$$

Following for instance Chap. 3, Sect. 8 of [16], the weak formulation of the above problem consists, given $f \in L^2(0,T;L^2(\Omega))$, $u_0 \in H_0^1(\Omega)$, $v_0 \in L^2(\Omega)$, in finding

$$u \in L^\infty(0,T;H_0^1(\Omega)),\ \frac{\partial u}{\partial t} \in L^\infty(0,T;L^2(\Omega)),\ \frac{\partial^2 u}{\partial t^2} \in L^2(0,T;H^{-1}(\Omega)),$$

such that $u(\cdot,0) = u_0$ in $H_0^1(\Omega)$, $\frac{\partial u}{\partial t}(\cdot,0) = v_0$ in $L^2(\Omega)$ and

$$\left\langle \frac{\partial^2 u}{\partial t^2}, v \right\rangle + \int_\Omega \nabla u \cdot \nabla v = \int_\Omega f v, \tag{4}$$

for all $v \in H_0^1(\Omega)$, *a.e.* $t \in (0,T)$, where $< \cdot, \cdot >$ denotes the duality pairing between $H^{-1}(\Omega)$ and $H_0^1(\Omega)$. From Chap. 3, Sect. 8, Theorem 8.1 and Remark 8.2 of [16], such a solution exists and is unique. Moreover, using a parabolic regularization technique, it is proved in Theorem 8.2 of [16] that

$$u \in \mathcal{C}^0([0,T];H_0^1(\Omega)),\ \frac{\partial u}{\partial t} \in \mathcal{C}^0([0,T];L^2(\Omega)).$$

We now consider a finite element discretization in space. We will derive an a posteriori error bound in the case when the same mesh is used between initial and final time. Therefore, the interpolation error due to the use of several meshes will not be considered from the theoretical point of view. However, the adaptive algorithm presented in section 5 will obviously make use of several meshes whenever needed. Moreover, numerical experiments seem to show that this interpolation error should not be neglected in the framework of the wave equation, eventhough previous studies have shown that the interpolation error is not relevant for parabolic problems, provided the number of remeshings does not depend on the mesh size and time step, see [20, 10, 17]. The estimation of this interpolation error is not an obvious task since non-conforming anisotropic meshes are involved and is therefore beyond the scope of the present paper.

For any $h > 0$, let $\mathcal{T}_h$ be a conformal finite element triangulation with triangles K having diameter $h_K \leq h$. We are looking forward to using triangles with large aspect ratio, thus the usual minimum angle condition will not be satisfied. In the sequel we adopt the notations of [11, 12] but those of [13, 14] could be used as well. Let $T_K : \hat{K} \to K$ be the mapping from the reference triangle $\hat{K}$ to the current element K and let Δ_K be the union of the neighbouring triangles sharing a vertex with K. The following two assumptions must be satisfied : i) the number of triangles belonging to Δ_K must be bounded above, uniformely with respect to h and ii) the diameter of $T_K^{-1}(\Delta_K)$ should be bounded above, uniformely with respect to h, which excludes meshes with large curvature, see for instance [20, 19] for examples.

Let V_h be the usual subspace of $H_0^1(\Omega)$ corresponding to continuous functions, piecewise linear and vanishing on the boundary. We denote by $r_h : \mathcal{C}^0(\bar{\Omega}) \to V_h$ the usual Lagrange interpolant. Then, assuming that the initial data u_0 and v_0 are $\mathcal{C}^0(\bar{\Omega})$, the finite element discretization of (4) is to find $u_h \in H^2(0,T;V_h)$ such that $u_h(0) = r_h u_0$, $\partial u_h(0)/\partial t = r_h v_0$ and

$$\int_\Omega \frac{\partial^2 u_h}{\partial t^2} v_h + \int_\Omega \nabla u_h \cdot \nabla v_h = \int_\Omega f v_h, \tag{5}$$

for all $v_h \in V_h$, *a.e.* $t \in (0,T)$.

In the sequel we derive anisotropic a posteriori error estimates in the same norm as for parabolic problems, namely the $L^2(0,T;H^1(\Omega))$ norm, which allows the same adaptive algorithm as in [20] to be used.

3 Anisotropic a posteriori error estimates

In order to control the error in the $L^2(0,T;H^1(\Omega))$ norm, we introduce as in [18] the elliptic reconstruction $U \in L^2(0,T;H_0^1(\Omega))$ defined by

$$\int_\Omega \frac{\partial^2 u_h}{\partial t^2} v + \int_\Omega \nabla U \cdot \nabla v = \int_\Omega f v, \tag{6}$$

Our goal is to control $u - u_h = u - U + U - u_h$.

We first recall some interpolation estimates due to [11, 12]. For any triangle K of the mesh, let $T_K : \hat{K} \to K$ be the affine transformation which maps the reference triangle $\hat{K}$ into K. Let M_K be the Jacobian of T_K that is

$$\mathbf{x} = T_K(\hat{\mathbf{x}}) = M_K \hat{\mathbf{x}} + \mathbf{t}_K.$$

Since M_K is invertible, it admits a singular value decomposition $M_K = R_K^T \Lambda_K P_K$, where R_K and P_K are orthogonal and where Λ_K is diagonal with positive entries. In the following we set

$$\Lambda_K = \begin{pmatrix} \lambda_{1,K} & 0 \\ 0 & \lambda_{2,K} \end{pmatrix} \qquad \text{and} \qquad R_K = \begin{pmatrix} \mathbf{r}_{1,K}^T \\ \mathbf{r}_{2,K}^T \end{pmatrix}, \tag{7}$$

with the choice $\lambda_{1,K} \geq \lambda_{2,K}$. Finally, for any triangle K of the mesh, the three edges will be denoted by $\ell_{i,K}$, $i = 1,2,3$.

The following interpolation estimates for the Clément interpolant R_h can be found in [11, 12, 22].

Lemma 1 *There is a constant C independent of the mesh size and aspect ratio such that, for all $v \in H^1(\Omega)$, for all $K \in \mathcal{T}_h$, for all $i = 1,2,3$:*

$$\|v - R_h v\|_{L^2(K)}^2 + \frac{\lambda_{1,K}\lambda_{2,K}}{|\ell_{i,K}|} \|v - R_h v\|_{L^2(\ell_{i,K})}^2 \leq C \omega_K^2(v), \tag{8}$$

where $\omega_K(v)$ is defined by

$$\omega_K^2(v) = \lambda_{1,K}^2 \Big(\mathbf{r}_{1,K}^T G_K(v) \mathbf{r}_{1,K} \Big) + \lambda_{2,K}^2 \Big(\mathbf{r}_{2,K}^T G_K(v) \mathbf{r}_{2,K} \Big), \tag{9}$$

and $G_K(v)$ denotes the 2×2 matrix defined by

$$G_K(v) = \begin{pmatrix} \displaystyle\int_{\Delta_K} \left(\frac{\partial v}{\partial x_1}\right)^2 dx & \displaystyle\int_{\Delta_K} \frac{\partial v}{\partial x_1}\frac{\partial v}{\partial x_2} dx \\ \displaystyle\int_{\Delta_K} \frac{\partial v}{\partial x_1}\frac{\partial v}{\partial x_2} dx & \displaystyle\int_{\Delta_K} \left(\frac{\partial v}{\partial x_2}\right)^2 dx \end{pmatrix}. \tag{10}$$

We are now in position to control the error $u - u_h = u - U + U - u_h$. Concerning $U - u_h$, we have the following result.

Lemma 2 *Let u_h, U be defined by (5), (6), respectively. Then, there exists C independent of the mesh size and aspect ratio such that*

$$\int_0^T \int_\Omega |\nabla(U - u_h)|^2 \leq C \int_0^T \sum_{K \in \mathcal{T}_h} \eta_{K,1}^2, \tag{11}$$

where $\eta_{K,1}^2$ is defined by

$$\eta_{K,1}^2 = \left(\left\| f - \frac{\partial^2 u_h}{\partial t^2} \right\|_{L^2(K)} + \frac{1}{2} \sum_{i=1}^{3} \left(\frac{|\ell_{i,K}|}{\lambda_{1,K}\lambda_{2,K}} \right)^{1/2} \| \left[\nabla u_h \cdot \mathbf{n}\right] \|_{L^2(\ell_{i,K})} \right) \times \omega_K(U - u_h). \tag{12}$$

Here $[\cdot]$ denotes the jump of the bracketed quantity across edge $\ell_{i,K}$, with the convention $[\cdot] = 0$ for an edge $\ell_{i,K}$ on the boundary $\partial\Omega$.

Proof. Using (6) and (5), we have

$$\int_\Omega |\nabla(U - u_h)|^2 = \int_\Omega \left(f - \frac{\partial^2 u_h}{\partial t^2} \right) (U - u_h - v_h) - \int_\Omega \nabla u_h \cdot \nabla (U - u_h - v_h) \qquad \forall v_h \in V_h.$$

Integrating by parts the diffusion term over each triangle K, choosing $v_h = R_h(U - u_h)$, the Clément interpolant of $U - u_h$ and using the interpolation estimates of Lemma 1 yields the result. □

Remark 1 *The estimator (12) is not a usual error estimator since $U - u_h$ is still involved. However, if we can guess $U - u_h$, then (11) can be used to derive a computable quantity. This idea has been used in [20, 22] and an efficient anisotropic error indicator has also been obtained replacing the derivatives*

$$\frac{\partial (U - u_h)}{\partial x_i} \text{ in (10) by } \Pi_h \frac{\partial u_h}{\partial x_i} - \frac{\partial u_h}{\partial x_i}, \ i=1,2, \tag{13}$$

where Π_h is the approximate $L^2(\Omega)$ projection onto V_h defined for each vertex P of $\mathcal{T}_h$ by

$$\begin{pmatrix} \Pi_h \left(\dfrac{\partial u_h}{\partial x_1}\right)(P) \\ \Pi_h \left(\dfrac{\partial u_h}{\partial x_2}\right)(P) \end{pmatrix} = \frac{1}{\displaystyle\sum_{\substack{K \in \mathcal{T}_h \\ P \in K}} |K|} \begin{pmatrix} \displaystyle\sum_{\substack{K \in \mathcal{T}_h \\ P \in K}} |K| \left(\frac{\partial u_h}{\partial x_1}\right)_{|K} \\ \displaystyle\sum_{\substack{K \in \mathcal{T}_h \\ P \in K}} |K| \left(\frac{\partial u_h}{\partial x_2}\right)_{|K} \end{pmatrix}.$$

We now control $u-U$ with respect to $U-u_h$.

Lemma 3 *Let u, u_h, U be defined by (4), (5), (6), respectively. Assume that $f \in H^2(0,T;L^2(\Omega))$ so that $u_h \in H^4(0,T;V_h)$ and $U \in H^2(0,T;H_0^1(\Omega))$. We have, for $0 \leq t \leq T$:*

$$\int_\Omega \left|\frac{\partial}{\partial t}(u-U)(t)\right|^2 + \int_\Omega |\nabla(u-U)(t)|^2$$
$$\leq 2\int_\Omega \left|\frac{\partial}{\partial t}(u-U)(0)\right|^2 + 2\int_\Omega |\nabla(u-U)(0)|^2 + 2t\int_0^t \int_\Omega \left|\frac{\partial^2}{\partial t^2}(U-u_h)\right|^2. \tag{14}$$

Proof. Using (4) and (6) we have

$$\int_\Omega \frac{\partial^2}{\partial t^2}(u-U)v + \int_\Omega \nabla(u-U)\cdot\nabla v = \int_\Omega \frac{\partial^2}{\partial t^2}(u_h-U)v,$$

for all $v \in H_0^1(\Omega)$, *a.e.* $t \in (0,T)$. We then choose $v = \partial/\partial t(u-U)$ to obtain

$$\frac{1}{2}\frac{d}{dt}\int_\Omega \left(\left|\frac{\partial}{\partial t}(u-U)\right|^2 + |\nabla(u-U)|^2\right) = \int_\Omega \frac{\partial^2}{\partial t^2}(u_h-U)\frac{\partial}{\partial t}(u-U).$$

We set

$$y(t) = \int_\Omega \left(\left|\frac{\partial}{\partial t}(u-U)\right|^2 + |\nabla(u-U)|^2\right),$$

and use Cauchy-Schwarz inequality to obtain

$$\frac{1}{2}\frac{d}{dt}y(t) \leq \left\|\frac{\partial^2}{\partial t^2}(u_h-U)\right\|_{L^2(\Omega)} y^{1/2}(t). \tag{15}$$

Since

$$\frac{d}{dt}y^{1/2} = \frac{1}{2}y^{-1/2}\frac{dy}{dt},$$

we therefore obtain, integrating (15) between time 0 and t :

$$y^{1/2}(t) \leq y^{1/2}(0) + \int_0^t \left\|\frac{\partial^2}{\partial t^2}(u_h-U)\right\|_{L^2(\Omega)}.$$

Taking the square and using Young's inequality yields the result. □

It now remains to estimate $\partial/\partial t(u-U)(0)$, $\nabla(u-U)(0)$ and $\partial^2/\partial t^2(U-u_h)$.

Lemma 4 *Assume that the polygon Ω is convex and that $f \in H^2(0,T;L^2(\Omega))$. Let u, u_h, U be defined by (4), (5), (6), respectively. Then, there exists C_1 independent of the mesh size (but depending on the aspect ratio) such that*

$$\int_0^T \int_\Omega \left|\frac{\partial^2}{\partial t^2}(U-u_h)\right|^2 \leq C_1 \int_0^T \sum_{K\in\mathcal{T}_h} \eta_{K,2}^2, \tag{16}$$

where $\eta^2_{K,2}$ *is defined by*

$$\eta^2_{K,2} = h_K^4 \left\| \frac{\partial^2 f}{\partial t^2} - \frac{\partial^4 u_h}{\partial t^4} \right\|^2_{L^2(K)} + h_K^3 \left\| \left[\nabla \frac{\partial^2 u_h}{\partial t^2}.n \right] \right\|^2_{L^2(\partial K)}. \qquad (17)$$

Moreover, if u_0, $v_0 \in H^2(\Omega)$, *then there exists* C_2 *independent of the mesh size and aspect ratio,* C_3 *and* C_4 *independent of the mesh size (but depending on the aspect ratio) such that*

$$\int_\Omega \left| \frac{\partial}{\partial t}(u-U)(0) \right|^2 + \int_\Omega |\nabla(u-U)(0)|^2$$
$$\leq C_2 \sum_{K\in\mathcal{T}_h} \eta^2_{K,3} + C_3 \sum_{K\in\mathcal{T}_h} \eta^2_{K,4} + C_4 h^2 \int_\Omega \left(|D^2 u_0|^2 + |D^2 v_0|^2 \right). \quad (18)$$

where $\eta^2_{K,3}$ *and* $\eta^2_{K,4}$ *are defined by*

$$\eta^2_{K,3} = \left(\left\| f(0) - \frac{\partial^2 u_h}{\partial t^2}(0) \right\|_{L^2(K)} + \frac{1}{2} \sum_{i=1}^{3} \left(\frac{|\ell_{i,K}|}{\lambda_{1,K}\lambda_{2,K}} \right)^{1/2} \| \left[\nabla u_h(0) \cdot \mathbf{n} \right] \|_{L^2(\ell_{i,K})} \right)$$
$$\times \omega_K((u-U)(0)), \qquad (19)$$

$$\eta^2_{K,4} = h_K^4 \left\| \frac{\partial f}{\partial t}(0) - \frac{\partial^3 u_h}{\partial t^3}(0) \right\|^2_{L^2(K)} + h_K^3 \left\| \left[\nabla \frac{\partial u_h}{\partial t}(0) \cdot \mathbf{n} \right] \right\|^2_{L^2(\partial K)}. \qquad (20)$$

Proof. We mimick [18] in order to obtain (17). From (5) and (6) we have

$$\int_\Omega \nabla(U-u_h) \cdot \nabla v_h = 0 \qquad \forall v_h \in V_h.$$

Since $f \in H^2(0,T;L^2(\Omega))$, $u_h \in H^4(0,T;V_h)$ and $U \in H^2(0,T;H^1_0(\Omega))$, thus, differentiating the above equation twice with respect to t, we obtain

$$\int_\Omega \nabla \frac{\partial^2}{\partial t^2}(U-u_h) \cdot \nabla v_h = 0 \qquad \forall v_h \in V_h. \qquad (21)$$

Let $\varphi \in L^2(0,T;H^1_0(\Omega))$ be defined by

$$\int_\Omega \nabla\varphi \cdot \nabla v = \int_\Omega \frac{\partial^2}{\partial t^2}(U-u_h) v \qquad \forall v \in H^1_0(\Omega).$$

We thus have, using (21),

$$\int_\Omega \left| \frac{\partial^2}{\partial t^2}(U-u_h) \right|^2 = \int_\Omega \nabla\varphi \cdot \nabla \frac{\partial^2}{\partial t^2}(U-u_h)$$
$$= \int_\Omega \nabla(\varphi - v_h) \cdot \nabla \frac{\partial^2}{\partial t^2}(U-u_h),$$

for all $v_h \in V_h$. Since Ω is a convex polygon, $U \in H^2(0,T;H^2(\Omega))$, thus we can integrate by parts the diffusion term over each triangle K to obtain

$$\int_\Omega \left| \frac{\partial^2}{\partial t^2}(U-u_h) \right|^2 = \sum_{K\in\mathcal{T}_h} \left(\int_K \Delta \frac{\partial^2}{\partial t^2}(U-u_h)(\varphi - v_h) + \frac{1}{2} \int_{\partial K} \left[\nabla \frac{\partial^2}{\partial t^2}(U-u_h) \cdot n \right] (\varphi - v_h) \right).$$

Since Ω is a convex polygon, $\varphi \in L^2(0,T;H^2(\Omega))$, we are thus allowed to choose $v_h = r_h\varphi$, the Lagrange interpolant of φ. Moreover, there exists C depending only on the size of Ω such that

$$\|\varphi\|_{H^2(\Omega)} \leq C \left\| \frac{\partial^2}{\partial t^2}(U-u_h) \right\|_{L^2(\Omega)}.$$

Therefore, using standart interpolation results, there exists C independent of the mesh size (but depending on the aspect ratio) such that

$$\int_\Omega \left| \frac{\partial^2}{\partial t^2}(U-u_h) \right|^2 \leq C \sum_{K\in\mathcal{T}_h} \left(h_K^4 \left\| \Delta \frac{\partial^2}{\partial t^2}(U-u_h) \right\|^2_{L^2(K)} + \frac{1}{2} h_K^3 \left\| \left[\nabla \frac{\partial^2}{\partial t^2}(U-u_h)\cdot n \right] \right\|^2_{L^2(\partial K)} \right).$$

Finally, since

$$-\Delta \frac{\partial^2 U}{\partial t^2} = \frac{\partial^2 f}{\partial t^2} - \frac{\partial^4 u_h}{\partial t^4} \qquad \text{and} \qquad \left[\nabla \frac{\partial^2}{\partial t^2} U \cdot n \right] = 0,$$

then (16) is proved.

We now derive an upper bound for $(u-U)(0)$. From (6) we have, for all $v \in H^1_0(\Omega)$,

$$\begin{aligned} \int_\Omega \nabla(u-U)\cdot\nabla v &= \int_\Omega \frac{\partial^2}{\partial t^2}(u_h-u)v \\ &= \int_\Omega \left(\frac{\partial^2 u_h}{\partial t^2} v - fv - \nabla u_h \cdot \nabla v \right) + \int_\Omega \nabla(u-u_h)\cdot\nabla v, \end{aligned}$$

thus using (5) we obtain :

$$\begin{aligned} &\int_\Omega \nabla(u-U)\cdot\nabla v \\ &\qquad = \int_\Omega \left(\frac{\partial^2 u_h}{\partial t^2}(v-v_h) - f(v-v_h) - \nabla u_h \cdot \nabla(v-v_h) \right) \\ &\qquad\qquad + \int_\Omega \nabla(u-u_h)\cdot\nabla v. \quad (22) \end{aligned}$$

At initial time, the above equation writes

$$\begin{aligned} \int_\Omega \nabla(u-U)(0)\cdot\nabla v = \int_\Omega \left(\frac{\partial^2 u_h}{\partial t^2}(0)(v-v_h) - f(0)(v-v_h) - \nabla u_h(0)\cdot\nabla(v-v_h) \right) \\ + \int_\Omega \nabla(u_0 - r_h u_0)\cdot\nabla v. \quad (23) \end{aligned}$$

We then choose $v = (u-U)(0)$, $v_h = R_h(u-U)(0)$, where R_h is Clément's interpolant, use the interpolation estimates of Lemma 1 to obtain

$$\int_\Omega |\nabla(u-U)(0)|^2 \leq C \sum_{K\in\mathcal{T}_h} \eta^2_{K,3} + \int_\Omega |\nabla(u_0 - r_h u_0)|^2,$$

where C does not depend on the mesh size and aspect ratio.

Differentiating (22) with respect to t yields, at initial time

$$\int_\Omega \nabla \frac{\partial}{\partial t}(u-U)(0)\cdot\nabla v = \int_\Omega \left(\frac{\partial^3 u_h}{\partial t^3}(0)(v-v_h) - \frac{\partial f}{\partial t}(0)(v-v_h) - \nabla \frac{\partial u_h}{\partial t}(0)\cdot\nabla(v-v_h) \right) + \int_\Omega \nabla(v_0 - r_h v_0)\cdot\nabla v, \quad (24)$$

for all $v \in H_0^1(\Omega)$ and $v_h \in V_h$. Let $\varphi \in H_0^1(\Omega)$ be defined by

$$\int_\Omega \nabla\varphi\cdot\nabla v = \int_\Omega \frac{\partial}{\partial t}(U-u)(0)v \qquad \forall v \in H_0^1(\Omega).$$

We then chose $v = \partial/\partial t(u-U)(0)$ and use (24) to obtain

$$\int_\Omega \left| \frac{\partial}{\partial t}(u-U)(0) \right|^2 = \int_\Omega \left(\frac{\partial^3 u_h}{\partial t^3}(0)(\varphi-v_h) - \frac{\partial f}{\partial t}(0)(\varphi-v_h) - \nabla \frac{\partial u_h}{\partial t}(0)\cdot\nabla(\varphi-v_h) \right) + \int_\Omega \nabla(v_0 - r_h v_0)\cdot\nabla\varphi.$$

We then choose $v_h = r_h\varphi$, the Lagrange interpolant of φ, and use standart interpolation results to prove (18). □

We now state the main result of the paper.

Theorem 1 *Assume that the polygon Ω is convex, that $u_0, v_0 \in H^2(\Omega)$ and $f \in H^2(0,T;L^2(\Omega))$. Let u, u_h, U be defined by (4), (5), (6), respectively. Let the error estimators $\eta_{K,1}$, $\eta_{K,2}$, $\eta_{K,3}$, $\eta_{K,4}$ be defined by (12), (17), (19), (20), respectively. Then, there exists C_1 independent of the mesh size and aspect ratio, C_2 independent of the mesh size (but depending on the aspect ratio) such that*

$$\int_0^T \int_\Omega |\nabla(u-u_h)|^2 \le C_1 \left(\int_0^T \sum_{K\in\mathcal{T}_h} \eta_{K,1}^2 + \sum_{K\in\mathcal{T}_h} \eta_{K,3}^2 \right) + C_2 \left(\int_0^T \sum_{K\in\mathcal{T}_h} \eta_{K,2}^2 + \sum_{K\in\mathcal{T}_h} \eta_{K,4}^2 + h^2 \int_\Omega \left(|D^2 u_0|^2 + |D^2 v_0|^2 \right) \right). \quad (25)$$

Proof. We have

$$\int_0^T \int_\Omega |\nabla(u-u_h)|^2 \le 2\int_0^T \int_\Omega |\nabla(u-U)|^2 + 2\int_0^T \int_\Omega |\nabla(U-u_h)|^2.$$

From Lemma 3 we have

$$\int_0^T \int_\Omega |\nabla(u-U)|^2 \le 2T \int_\Omega \left| \frac{\partial}{\partial t}(u-U)(0) \right|^2 + 2T \int_\Omega |\nabla(u-U)(0)|^2 + T^2 \int_0^T \int_\Omega \left| \frac{\partial^2}{\partial t^2}(U-u_h) \right|^2.$$

Using Lemma 2 and 4 in the two above estimates yields the result. □

4 Time discretization and numerical results with non adapted meshes

The time discretization considered here corresponds to the implicit order two Newmark scheme. Given an integer N, we set $\tau = T/N$ the time step, $t^n = n\tau$ and introduce u_h^n an approximation of $u_h(t^n)$, $n = 0, ..., N$. The initial conditions are set to $u_h^0 = r_h u_0$, $v_h^0 = r_h v_0$. The first approximation $u_h^1 \in V_h$ satisfies

$$\int_\Omega \frac{u_h^1 - u_h^0 - \tau v_h^0}{\tau^2} v_h + \int_\Omega \left(\frac{1}{4} \nabla u_h^1 + \frac{1}{4} \nabla u_h^0 \right) \cdot \nabla v_h = \int_\Omega f(t^0) v_h,$$

for all $v_h \in V_h$. Then, for each $n = 1..., N$, we compute $u_h^{n+1} \in V_h$ such that

$$\int_\Omega \frac{u_h^{n+1} - 2u_h^n + u_h^{n-1}}{\tau^2} v_h + \int_\Omega \left(\frac{1}{4} \nabla u_h^{n+1} + \frac{1}{2} \nabla u_h^n + \frac{1}{4} \nabla u_h^{n-1} \right) \cdot \nabla v_h = \int_\Omega f(t^n) v_h,$$

for all $v_h \in V_h$. This scheme is $O(h + \tau^2)$ convergent in the $L^2(0, T; H^1(\Omega))$ norm. Therefore, setting $\tau = O(h)$, the error due to time discretization becomes asymptotically negligible so that the error due to space discretization only should be recovered. The interested reader should note that the Stormer-Numerov scheme [23] could be used to obtain a $O(h + \tau^4)$ convergent scheme.

We now report numerical results using uniform meshes and constant time steps when using

$$\int_0^T \sum_{K \in \mathcal{T}_h} \eta_{K,1}^2 \tag{26}$$

as error indicator. Going back to the upper bound (25), it can be noticed that the terms

$$\int_0^T \sum_{K \in \mathcal{T}_h} \eta_{K,2}^2 + \sum_{K \in \mathcal{T}_h} \eta_{K,4}^2$$

are of higher order and can thus be disregarded. This is not the case of the terms

$$\sum_{K \in \mathcal{T}_h} \eta_{K,3}^2 \qquad \text{and} \qquad h^2 \int_\Omega \left(|D^2 u_0|^2 + |D^2 v_0|^2 \right).$$

Since a trapezoidal quadrature formula is used to approximate (26), The $\eta_{K,3}$ term yields a contribution which is very similar to that of (26). Numerical results reported hereafter indicate that using (26) is indeed sufficient to represent correctly the error.

In order to study the quality of our error indicator, the following two effectivity indices are introduced

$$ei^{ZZ} = \left(\frac{\displaystyle\int_0^T \sum_{K\in\mathcal{T}_h} \left(\left| (I-\Pi_h)\left(\frac{\partial u_h}{\partial x_1}\right)\right|^2 + \left| (I-\Pi_h)\left(\frac{\partial u_h}{\partial x_2}\right)\right|^2 \right)}{\displaystyle\int_0^T \int_\Omega |\nabla(u-u_{h\tau})|^2} \right)^{1/2},$$

$$ei^{A} = \left(\frac{\displaystyle\int_0^T \sum_{K\in\mathcal{T}_h} \eta_{K,1}^2}{\displaystyle\int_0^T \int_\Omega |\nabla(u-u_{h\tau})|^2} \right)^{1/2},$$

where Π_h is defined in Remark 1, $\eta_{K,1}$ is defined in (12) and $u_{h\tau}$ denotes the continuous, piecewise linear approximation in time defined by

$$u_{h\tau}(x,t) = \frac{t-t^{n-1}}{\tau} u_h^n(x) + \frac{t^n - t}{\tau} u_h^{n-1}(x) \qquad t^{n-1} \le t \le t^n, \quad x \in \Omega. \quad (27)$$

The first numerical example corresponds to the case when

$$\Omega =]0,1[^2, \quad T = 0.4, \quad f(x_1,x_2,t) = 0,$$
$$u_0(x_1,x_2) = exp^{-1000*(x_1-0.5)^2}, \quad v_0(x_1,x_2) = 0. \quad (28)$$

Homogeneous boundary conditions apply on the vertical sides of Ω whereas Neuman homogeneous boundary conditions apply on the horizontal sides. Therefore the solution is one-dimensional and is given by d'Alembert formula

$$u(x_1,x_2,t) = \frac{1}{2}\Big(u_0(x_1-t,x_2) + u_0(x_1+t,x_2) \Big).$$

The computed solution at time 0 and 0.3 is reported in Fig. 1 when using a uniform mesh with mesh $h_x = 0.005$, $h_y = 0.05$ and a time step $\tau = 0.0005$. Numerical experiments with several uniform meshes and constant time steps are reported in Table 1.

In rows 1-6, it is observed that when setting $h = O(\tau^2)$ then the error is divided by four each time the time step is divided by two thus

$$\left(\int_0^T \int_\Omega |\nabla(u-u_{h\tau})|^2 \right)^{1/2} = O(h+\tau^2).$$

It should be noted that ei^{ZZ}, the effectivity index of ZZ, is not close to one in rows 1-3 due to the fact that the error due to space discretization is of the same order than the error due to time discretization.

In order to insure that the error due to time discretization becomes negligible with respect to the error due to space discretization we choose $\tau = O(h)$ in rows 7-9. We observe that the error is still of order one and that ei^{ZZ} now converges to one when h converges to zero, as for elliptic problems.

h_x	h_y	τ	e	ei^{ZZ}	ei^{A}	N_{vert}
0.01	0.1	0.01	1.70	0.23	0.60	1292
0.0025	0.025	0.005	0.46	0.19	0.52	20001
0.000625	0.00625	0.0025	0.11	0.19	0.51	325302
0.01	0.1	0.001	0.83	0.51	1.34	1292
0.0025	0.025	0.0005	0.10	0.86	2.41	20001
0.000625	0.00625	0.00025	0.022	0.98	2.67	325302
0.01	0.1	0.001	0.83	0.51	1.34	1292
0.005	0.05	0.0005	0.27	0.71	2.00	5070
0.0025	0.025	0.00025	0.10	0.87	2.44	20001
0.00125	0.0125	0.000125	0.046	0.96	2.63	80391

Table 1: Example 28. Non adapted meshes. $\tau^2 = O(h)$ and $\tau = O(h)$. Notation : $e = \left(\int_0^T \int_\Omega |\nabla(u - u_{h\tau})|^2\right)^{1/2}$, N_{vert} is the number of vertices of the final mesh.

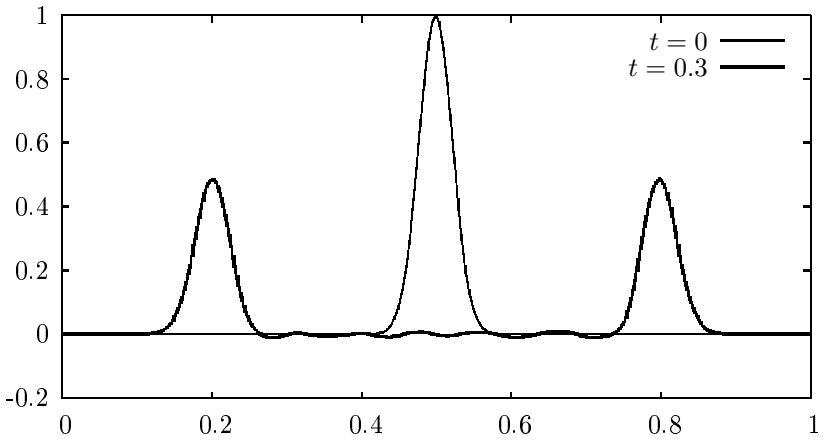

Figure 1: Example 28. Non adapted meshes. $h_x = 0.005$, $h_y = 0.05$, $\tau = 0.0005$. Computed solution $u_h(x_1, 1, t)$ with respect to x_1 at time $t = 0$ and $t = 0.3$.

In the second numerical example we change the following parameters in (28) :

$$T = 1.4, \quad u_0(x_1, x_2) = exp^{-1000*\left((x_1-0.5)^2+(x_2-0.5)^2\right)}, \tag{29}$$

and homogeneous boundary conditions apply on the whole boundary of Ω. For this test case, the exact solution is not known and multiple reflections can be observed when the initial wave hits the boundary, see Fig. 2.

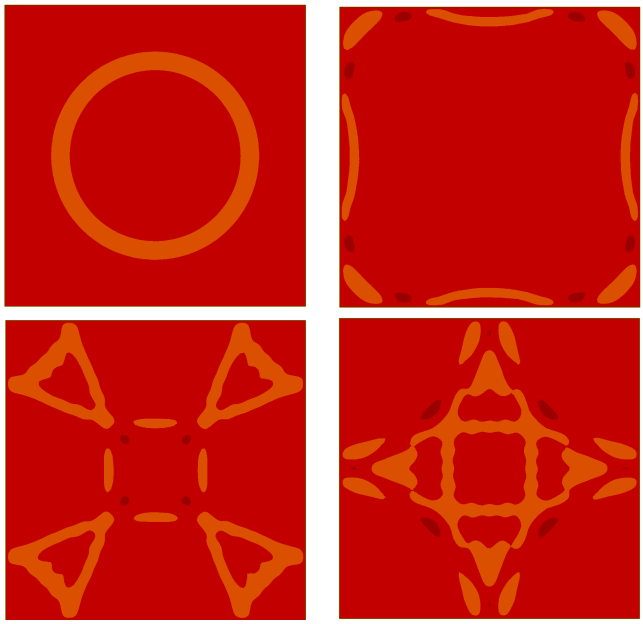

Figure 2: Example 29. Non adapted meshes. Numerical solution on a 100×100 uniform mesh at time 0.3, 0.6, 0.9, 1.2.

5 An anisotropic, adaptive finite element algorithm

We now use the adaptive algorithm described in [20] using

$$\int_0^T \sum_{K \in \mathcal{T}_h} \eta_{K,1}^2$$

as error indicator. The goal is to find anisotropic triangulations $\mathcal{T}_h^n$, $n = 1, ..., N$ such that the relative estimated error is close to a preset tolerance TOL, namely :

$$(1-\alpha)TOL \leq \frac{\left(\int_0^T \sum_{K \in \mathcal{T}_h} \eta_{K,1}^2 \right)^{1/2}}{\left(\int_0^T \int_\Omega |\nabla u_{h\tau}|^2 \right)^{1/2}} \leq (1+\alpha)TOL. \tag{30}$$

Hereabove, $0 < \alpha < 1$ is a parameter affecting the number of remeshings, in general we choose $\alpha = 0.25$. A sufficient condition to satisfy (30) is to build, for each $n = 1, ..., N$, an anisotropic triangulation $\mathcal{T}_h^n$ such that

$$(1-\alpha)^2 TOL^2 \int_{t^{n-1}}^{t^n} \int_\Omega |\nabla u_{h\tau}|^2 \leq \int_{t^{n-1}}^{t^n} \sum_{K \in \mathcal{T}_h} \eta_{K,1}^2 \leq (1+\alpha)^2 TOL^2 \int_{t^{n-1}}^{t^n} \int_\Omega |\nabla u_{h\tau}|^2.$$

We then proceed as in [20] to build such an anisotropic mesh, using the `BL2D` mesh generator [9].

Example (28) is considered. Unless otherwise specified, the initial triangulation is a uniform 100×10 mesh. Results are reported when using several values of TOL with $\tau = O(TOL^{-1})$ so that the error due to time discretization becomes asymptotically negligible. The results of Table 2 correspond to the choice $\alpha = 0.25$ in (30) which was the parameter used in [20]. As expected, the error is divided by two each time TOL is, the number of vertices of the final mesh is multiplied by four and the number of remeshings is roughly constant. However, unlike the results obtained with non adapted meshes, the effectivity index of ZZ does not go to one. The results with $TOL = 0.125$ are reported in Fig. 3 to 5. As seen in Fig. 5, the discrepancy between the true and estimated error increases with respect to time. We suspect that the missing error is due to interpolation between meshes and therefore we perform experiments with $\alpha = 0.5$ in (30), or even by imposing the times at which remeshing is performed. The results are reported in Table 3. Clearly, the effectivity index of ZZ at final time depends on the number of remeshings. Therefore, unlike what has been observed for parabolic problems [20, 17], we conjecture that the interpolation error between meshes cannot be neglected for the wave equation. Estimating this error is not an easy task for non compatible anisotropic meshes and is beyond the scope of the present paper. However, this interpolation error should be considered in a forthcoming contribution.

TOL	τ	e	ei^{ZZ}	ei^{A}	N_{vert}	N_{mesh}	*max ratio*	*av ratio*
0.125	0.001	0.27	0.45	1.23	2382	28	145	27
0.0625	0.0005	0.10	0.64	1.73	9781	27	245	29
0.03125	0.00025	0.051	0.64	1.77	36865	39	226	30
0.015625	0.000125	0.023	0.71	1.96	182914	45	285	25

Table 2: Example 28. Adaptive algorithm. Results with respect to TOL when $\alpha = 0.25$. Caption : N_{mesh} is the number of generated meshes, *max ratio* (resp. *av ratio*) is the maximum (resp. average) aspect ratio $\lambda_{1,K}/\lambda_2 K$ of the final mesh.

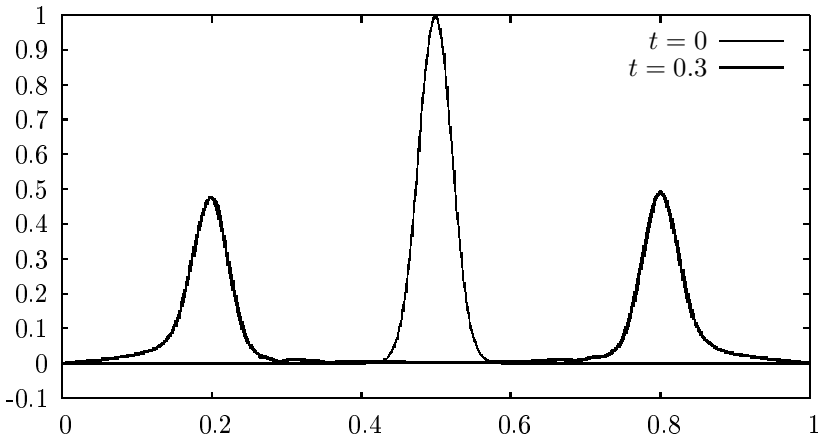

Figure 3: Example 28. Adaptive algorithm with $TOL = 0.125$, $\alpha = 0.25$. Computed solution $u_h(x_1, 1, t)$ with respect to x_1 at time $t = 0$ and $t = 0.3$.

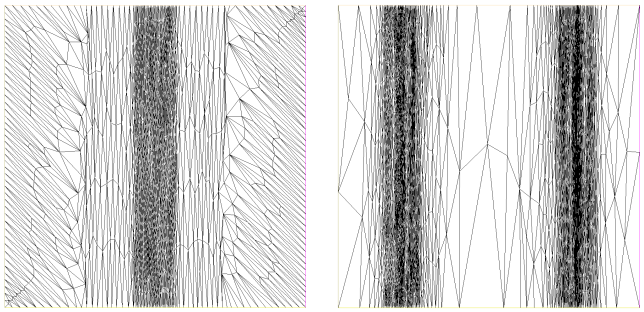

Figure 4: Example 28. Adaptive algorithm with $TOL = 0.125$, $\alpha = 0.25$. Adapted mesh at time $t = 0$ (1305 vertices) and $t = 0.3$ (2164 vertices).

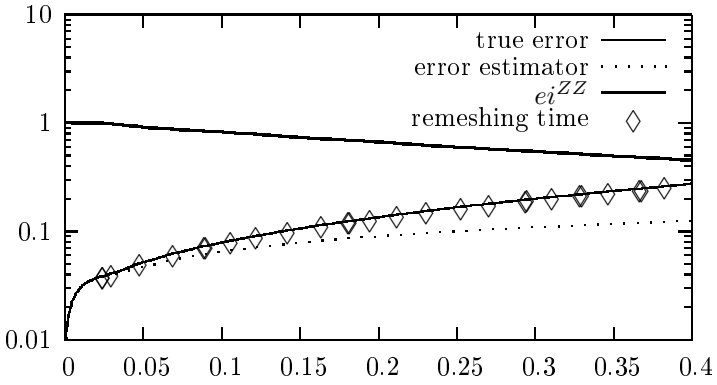

Figure 5: Example 28. Adaptive algorithm with $TOL = 0.125$, $\alpha = 0.25$. True and estimated error with respect to time.

e	ei^{ZZ}	ei^{A}	N_{vert}	N_{mesh}	*max ratio*	*av ratio*
0.049	0.77	2.06	60179	23	217	26
0.051	0.64	1.77	36865	39	226	30
0.071	0.76	2.03	33281	20	204	34
0.064	0.68	1.85	15817	40	355	56

Table 3: Example 28. Adapted meshes. Influence of the number of remeshings with $TOL = 0.03125$ and $\tau = 0.00025$; row 1 : adaptive algorithm with $\alpha = 0.5$; row 2 : adaptive algorithm with $\alpha = 0.25$; row 3 : 20 imposed remeshings at time 0.02, 0.04,... 0.38; row 4 : 40 imposed remeshings at time 0.01, 0.02,... 0.39.

In order to check the conjecture that the interpolation error between meshes cannot be neglected, conservative interpolation [4] rather than linear interpolation is considered to interpolate the computed solution after remeshing. The results are reported in Table 4 and clearly show that the effectivity index of ZZ is closer to one with conservative interpolation rather than linear interpolation.

TOL	τ	e	ei^{ZZ}	ei^{A}	N_{vert}	N_{mesh}	*max ratio*	*av ratio*
0.125	0.001	0.20	0.66	1.77	3797	18	111	24
0.0625	0.0005	0.089	0.74	2.00	9260	25	245	32
0.03125	0.00025	0.045	0.73	2.00	27711	37	339	43
0.015625	0.000125	0.021	0.78	2.15	86381	46	799	52

Table 4: Example 28. Adaptive algorithm. Results with respect to TOL when $\alpha = 0.25$ when using the conservative interpolation method of [4] to interpolate the computed solution after remeshing.

Still in order to check the conjecture that the interpolation error between meshes cannot be neglected, the damped wave equation is considered

$$\frac{\partial^2 u}{\partial t^2} - \Delta u + \beta \frac{\partial u}{\partial t} = f. \tag{31}$$

Clearly, when the damping coefficient $\beta \geq 0$ increases, then the behaviour of the equation ressembles that of a parabolic problem, thus we conjecture that the interpolation error between meshes should decrease. Still considering the example (28) of the previous section, the exact solution can be computed by means of Fourier series. The adaptive algorithm is run with several values of β and the results are reported in Table 5. Clearly, when $\beta = 100$, then the effectivity index of ZZ is close to one and the effectivity index of our error estimator is close to 2.7 which corresponds to the value already observed for various elliptic and parabolic problems, which shows that the interpolation error between meshes becomes unimportant.

β	e	ei^{ZZ}	ei^{A}	N_{vert}	N_{mesh}	*max ratio*	*av ratio*
0.	0.27	0.45	1.23	2382	28	145	27
10.	0.098	0.68	1.86	2264	30	141	27
100.	0.060	0.99	2.73	233	8	175	44

Table 5: Example 28. Adaptive algorithm. Results when solving the damped wave equation (31) with several values of β with $TOL = 0.125$ and $\tau = 0.001$.

Example (29) of the previous section is now considered. Eventhough the exact solution is not known, convergence of the adaptive algorithm with respect to TOL is observed. The adapted meshes at time 0.3, 0.6, 0.9 and 1.2 are reported in Fig. 6. Plots of the solution along the diagonal are reported in Fig. 7 and 8 for several values of TOL. The results are summarized in Table 6.

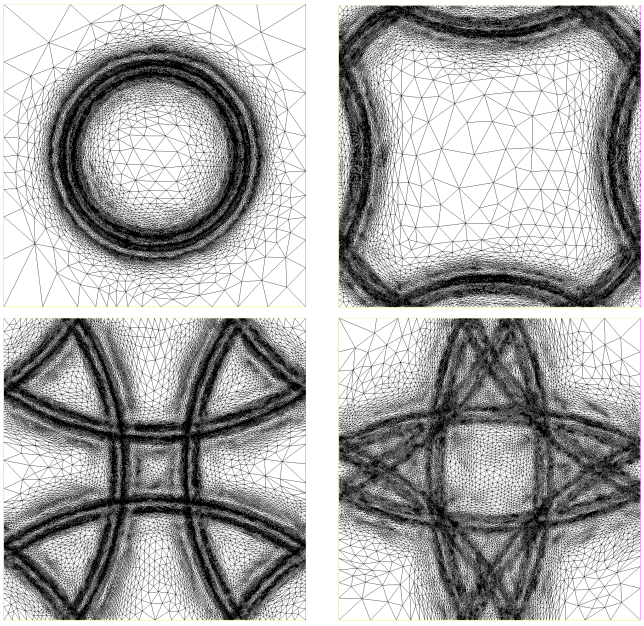

Figure 6: Example 29. Adaptive algorithm with $TOL = 0.125$. Adapted mesh at time 0.3 (23632 vertices), 0.6 (37132 vertices), 0.9 (38187 vertices), 1.2 (52132 vertices).

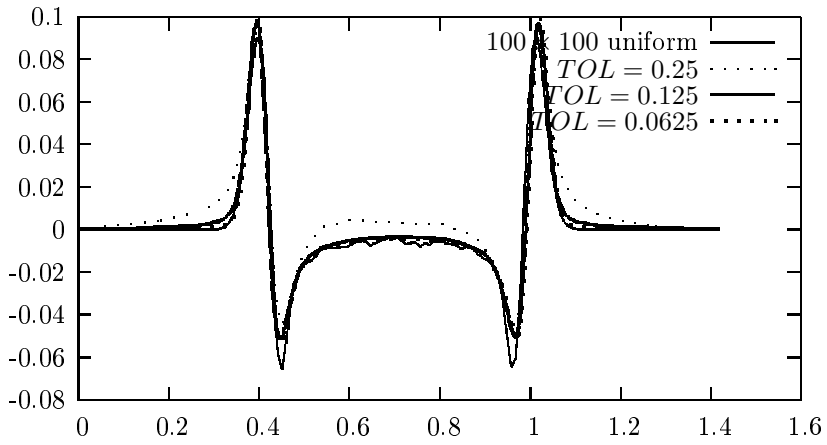

Figure 7: Example 29. Adaptive algorithm. Computed solution $u_h(x_1, x_2, t)$ along the diagonal $x_1 = x_2$ at time 0.3. Convergence with respect to TOL when $\tau = 0.001$.

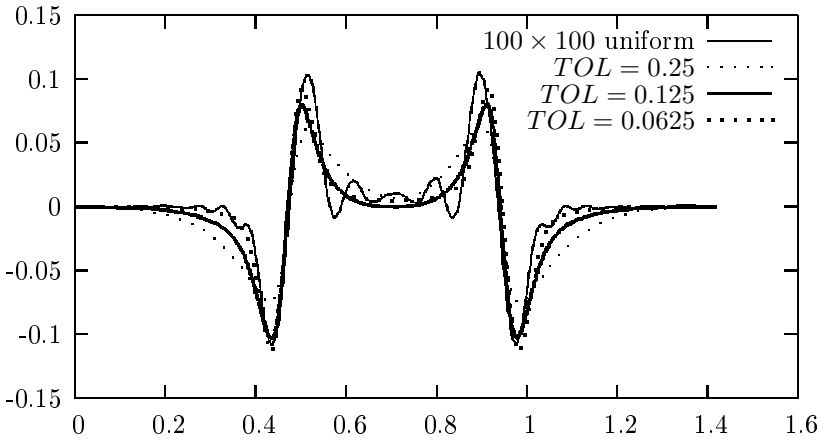

Figure 8: Example 29. Adaptive algorithm. Computed solution $u_h(x_1, x_2, t)$ along the diagonal $x_1 = x_2$ at time 1.2. Convergence with respect to TOL when $\tau = 0.001$.

TOL	τ	N_{vert}	N_{mesh}	*max ratio*	*av ratio*
0.25	0.001	7172	104	12	2
0.125	0.001	50264	146	38	3
0.0625	0.001	176427	160	58	4

Table 6: Example 29. Adaptive algorithm. Results with respect to TOL.

6 Conclusions

An a posteriori error estimate in the $L^2(0,T;H^1(\Omega))$ norm is proposed for the wave equation. Numerical results on non-adapted meshes show that the error indicator $\eta_{K,1}$ defined by (12) is sharp even with meshes having large aspect ratio. An adaptive algorithm already presented for parabolic problems is considered. A numerical study of the effectivity index on adapted meshes shows a discrepancy between the true error and the error indicator. We suspect that this error corresponds to the interpolation error introduced when remeshing occurs. Experiments of the damped wave equation indeed show that the discrepancy between error and estimator decreases when the damping coefficient increases. This is in accordance with the fact that the interpolation error due to remeshing does not need to be considered for parabolic problems provided the number of remeshings does not depend on h (or TOL) and τ, see [20, 10, 17].

An estimation of the interpolation error due to remeshing should be the subject of a future work. This is a difficult task since non-compatible anisotropic meshes are involved.

Acknowledgements

Georgios Akrivis is acknowledged for constructive remarks. Frédéric Alauzet is acknowledged for providing the program corresponding to conservative interpolation [4].

References

[1] S. Adjerid. A posteriori finite element error estimation for second-order hyperbolic problems. *Comput. Methods Appl. Mech. Engrg.*, 191(41-42):4699–4719, 2002.

[2] S. Adjerid. A posteriori error estimation for the method of lumped masses applied to second-order hyperbolic problems. *Comput. Methods Appl. Mech. Engrg.*, 195(33-36):4203–4219, 2006.

[3] F. Alauzet, P. J. Frey, P. L. George, and B. Mohammadi. 3D transient fixed point mesh adaptation for time-dependent problems: application to CFD simulations. *J. Comput. Phys.*, 222(2):592–623, 2007.

[4] F. Alauzet and M. Mehrenberger. P1-conservative solution interpolation on unstructured triangular meshes. *Rapport de Recherche INRIA No 8604*, 2009.

[5] W. Bangerth and R. Rannacher. Finite element approximation of the acoustic wave equation: error control and mesh adaptation. *East-West J. Numer. Math.*, 7(4):263–282, 1999.

[6] W. Bangerth and R. Rannacher. Adaptive finite element techniques for the acoustic wave equation. *J. Comput. Acoust.*, 9(2):575–591, 2001.

[7] Y. Belhamadia, A. Fortin, and E. Chamberland. Three-dimensional anisotropic mesh adaptation for phase change problems. *J. Comput. Phys.*, 201(2):753–770, 2004.

[8] C. Bernardi and E. Süli. Time and space adaptivity for the second-order wave equation. *Math. Models Methods Appl. Sci.*, 15(2):199–225, 2005.

[9] H. Borouchaki and P. Laug. The BL2D mesh generator: Beginner's guide, user's and programmer's manual. Technical Report RT-0194, Institut National de Recherche en Informatique et Automatique (INRIA), Rocquencourt, 78153 Le Chesnay, France, 1996.

[10] E. Burman and M. Picasso. Anisotropic, adaptive finite elements for the computation of a solutal dendrite. *Interfaces Free Bound.*, 5(2):103–127, 2003.

[11] L. Formaggia and S. Perotto. New anisotropic a priori error estimates. *Numer. Math.*, 89(4):641–667, 2001.

[12] L. Formaggia and S. Perotto. Anisotropic error estimates for elliptic problems. *Numer. Math.*, 94:67–92, 2003.

[13] G. Kunert. An a posteriori residual error estimator for the finite element method on anisotropic tetrahedral meshes. *Numer. Math.*, 86(3):471–490, 2000.

[14] G. Kunert and R. Verfürth. Edge residuals dominate a posteriori error estimates for linear finite element methods on anisotropic triangular and tetrahedral meshes. *Numer. Math.*, 86(2):283–303, 2000.

[15] X. D. Li and N.-E. Wiberg. Implementation and adaptivity of a space-time finite element method for structural dynamics. *Comput. Methods Appl. Mech. Engrg.*, 156(1-4):211–229, 1998.

[16] J.-L. Lions and E. Magenes. *Non-homogeneous boundary value problems and applications. Vol. I.* Springer-Verlag, New York, 1972. Translated from the French by P. Kenneth, Die Grundlehren der mathematischen Wissenschaften, Band 181.

[17] A. Lozinski, V. Prachittham, and M. Picasso. An anisotropic error estimator for the crank-nicolson method: application to a parabolic problem. *SIAM J. Sci. Comp.*, 31(4):2757–2783, 2009.

[18] C. Makridakis and R. H. Nochetto. Elliptic reconstruction and a posteriori error estimates for parabolic problems. *SIAM J. Numer. Anal.*, 41(4):1585–1594 (electronic), 2003.

[19] S. Micheletti, S. Perotto, and M. Picasso. Stabilized finite elements on anisotropic meshes: a priori error estimates for the advection-diffusion and the Stokes problems. *SIAM J. Numer. Anal.*, 41(3):1131–1162, 2003.

[20] M. Picasso. An anisotropic error indicator based on Zienkiewicz-Zhu error estimator : application to elliptic and parabolic problems. *SIAM J. Sci. Comp.*, 24:1328–1355, 2003.

[21] M. Picasso. Numerical study of the effectivity index for an anisotropic error indicator based on Zienkiewicz-Zhu error estimator. *Comm. Numer. Methods Engrg.*, 19(1):13–23, 2003.

[22] M. Picasso. Adaptive finite elements with large aspect ratio based on an anisotropic error estimator involving first order derivatives. *Comput. Methods Appl. Mech. Engrg.*, 196(1-3):14–23, 2006.

[23] J. Stoer and R. Bulirsch. *Introduction to numerical analysis*, volume 12 of *Texts in Applied Mathematics*. Springer-Verlag, New York, third edition, 2002. Translated from the German by R. Bartels, W. Gautschi and C. Witzgall.

Centre de recherche INRIA Paris – Rocquencourt
Domaine de Voluceau - Rocquencourt - BP 105 - 78153 Le Chesnay Cedex (France)

Centre de recherche INRIA Bordeaux – Sud Ouest : Domaine Universitaire - 351, cours de la Libération - 33405 Talence Cedex
Centre de recherche INRIA Grenoble – Rhône-Alpes : 655, avenue de l'Europe - 38334 Montbonnot Saint-Ismier
Centre de recherche INRIA Lille – Nord Europe : Parc Scientifique de la Haute Borne - 40, avenue Halley - 59650 Villeneuve d'Ascq
Centre de recherche INRIA Nancy – Grand Est : LORIA, Technopôle de Nancy-Brabois - Campus scientifique
615, rue du Jardin Botanique - BP 101 - 54602 Villers-lès-Nancy Cedex
Centre de recherche INRIA Rennes – Bretagne Atlantique : IRISA, Campus universitaire de Beaulieu - 35042 Rennes Cedex
Centre de recherche INRIA Saclay – Île-de-France : Parc Orsay Université - ZAC des Vignes : 4, rue Jacques Monod - 91893 Orsay Cedex
Centre de recherche INRIA Sophia Antipolis – Méditerranée : 2004, route des Lucioles - BP 93 - 06902 Sophia Antipolis Cedex

Éditeur
INRIA - Domaine de Voluceau - Rocquencourt, BP 105 - 78153 Le Chesnay Cedex (France)
http://www.inria.fr
ISSN 0249-6399